International Journal of Power Electronics and Drive System (IJPEDS)
Vol. 17, No. 1, March 2026, pp. 709~719
ISSN: 2088-8694, DOI: 10.11591/ijpeds.v17.i1.pp709-719

Optimizing small-scale geothermal power: insights from long-term testing and system modifications of a 3 MW geothermal condensing power plant in Kamojang, Indonesia

Lina Agustina, Suyanto, Budi Ismoyo
Research Center for Energy Conversion Technology, National Research and Innovation Agency of the Republic of Indonesia, South Tangerang, Indonesia

Article Info

Article history:

Received Jun 25, 2025
Revised Dec 18, 2025
Accepted Jan 23, 2026

Keywords:

Condenser vacuum
Condensing turbine
Geothermal power plant
Pilot plant performance
Specific steam consumption

ABSTRACT

This study presents the design, development, and performance evaluation of a 3 MW geothermal pilot power plant in Kamojang, Indonesia, developed by retrofitting a 2 MW backpressure turbine into a six-stage condensing turbine. With a 63.81% local content, the plant serves as one of Indonesia's first demonstrations of small-scale condensing turbine technology. Multi-phase testing yielded a maximum net output of 2.2 MW, below the design target due to condenser vacuum inefficiencies, strainer pressure losses, and reduced turbine isentropic efficiency. Subsequent condenser and strainer modifications improved vacuum stability, reduced pressure drops, and enhanced specific steam consumption (SSC) and overall performance. Exergy analysis identified the condenser (16.1%) and turbine (9.5%) as the primary sources of exergy destruction, resulting in an overall exergy efficiency of 73.6%, higher than typical small-scale geothermal benchmarks. While operational performance improved significantly, sustaining long-term vacuum stability and optimizing turbine operation under variable steam conditions remain key challenges. Future work should focus on automated vacuum control, real-time monitoring, and advanced thermodynamic–electrical optimization to enhance system reliability. This study provides practical insights into turbine retrofitting, condenser stabilization, and integrated exergy evaluation, contributing to the advancement and localization of small-scale geothermal power technology in Indonesia.

Corresponding Author:

Lina Agustina
Research Center for Energy Conversion Technology
National Research and Innovation Agency of the Republic of Indonesia
BJ Habibie Science & Technology Park, Puspiptek Raya St, South Tangerang
Banten Province 15314, Indonesia
Email: lina007@brin.go.id

1. INTRODUCTION

Global energy demand continues to rise, while reliance on fossil fuels drives resource depletion, price instability, and environmental impacts [1], [2]. Geothermal energy offers a sustainable, low-carbon, and base-load alternative with substantial global potential [2], [3]. Indonesia, endowed with 23 GW of geothermal resources across 357 sites, ranks second worldwide with 2.418 GW of installed capacity as of 2023 [4], [5]. National policies such as Law No. 27/2003 and Government Regulation No. 59/2007 target geothermal contributions exceeding 5% of the 2025 energy mix [6], [7].

Despite progress in large-scale geothermal development, small-scale plants (<10 MW) remain limited. These systems are essential for rural electrification and flexible grid integration but face technical and economic challenges [8]. Click or tap here to enter text.. Although condensing turbine technology is widely applied in geothermal plants [9], its adaptation, performance validation, and long-term operation in small-scale units—particularly those developed through local manufacturing or reverse engineering—are scarcely documented. The lack of field-scale performance data, subsystem modification insights, and integrated exergy evaluation creates a knowledge gap that hinders broader deployment of small-scale condensing systems in Indonesia.

This study addresses these gaps by examining the design, development, and operational performance of a 3 MW pilot geothermal power plant in Kamojang, West Java, developed through reverse engineering of a 2 MW backpressure turbine and achieving 63.81% local content [10]. The novelty lies in the first long-term experimental validation of a locally engineered small-scale condensing turbine under real geothermal conditions, supported by multi-year supervisory control and data acquisition (SCADA) monitoring, subsystem retrofit evaluation (strainer, condenser, and non-condensable gas (NCG) handling), and integrated thermodynamic–electrical exergy analysis. The findings support Indonesia's local manufacturing capability, expand pathways for rural electrification, and contribute to the nation's geothermal clean-energy transition

2. METHOD

2.1. Plant configuration

Figure 1 shows the process flow and design parameters of the 3 MW Kamojang geothermal pilot plant, while Table 1 presents its operating conditions. The Kamojang field is a steam-dominated reservoir (177–253.4 °C) utilizing a direct dry steam cycle [11], [12]. Steam from the production well is throttled from 12 bar(a) to 7 bar(a) via a restriction orifice, then separated from particulates in a demister/separator. Most steam expands through the six-stage condensing turbine, while a small portion is supplied to the ejector system and gland seals. Exhaust steam is condensed in a direct-contact condenser (0.16 bar abs), and the condensate is pumped to the cooling tower, where it is cooled by air through evaporative heat exchange before recirculation. This configuration maintains system efficiency under variable ambient conditions [13].

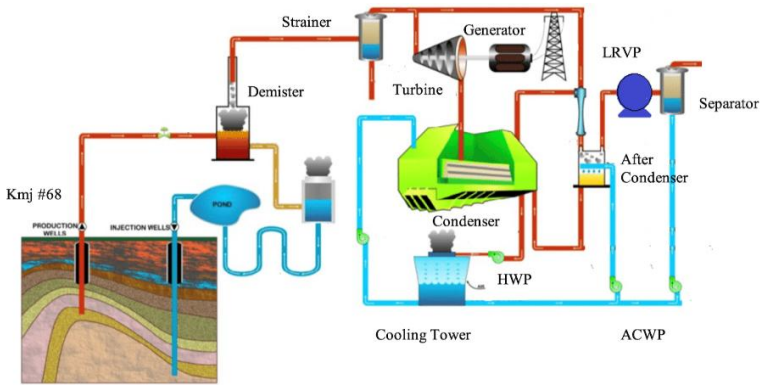

Figure 1. Flowchart of the process and design parameters of the 3 MW Kamojang GPP

Table 1. The process condition of the 3 MW Kamojang GPP referring to Figure 1

Parameter	Well head	Separator	Inlet turbine	Outlet turbine
Pressure, bar(a)	12	7	6.5	0.16
Temperature, °C	188	165	162	55.3
Steam flowrate, kg/s	8.3	8.3	7.6	7.6

2.2. Experimental setup

Figure 2 shows the powerhouse and turbine island of the 3 MW Kamojang geothermal plant, developed through reverse engineering of a 2 MW backpressure turbine from the Sibayak field. The original five-stage, 6,543 rpm turbine was converted into a six-stage condensing turbine designed for 0.16 bar(a) exhaust pressure and coupled via a gearbox to a 1,500 rpm, 3 MW synchronous generator. The plant consists

of the steam supply system, turbine-generator train, condenser, and cooling circuit, and the electrical control and monitoring subsystem [15].

Steam from well KMJ-68 (12–14 bar) is throttled and stabilized at approximately 5.65 bar(a) before entering the turbine, which operates at 6,485 rpm. Generator excitation is controlled by a Basler DEC-200 automatic voltage regulator (AVR) and protected by a GE SR-489 relay. Torque and rotational speed are measured using Kistler and Keyphasor® sensors. The single-pass SS-304 condenser operates near 0.16 bar(a) with a cooling-water flow rate of 7.3×10^6 kg/h, while non-condensable gases are removed using a hybrid ejector–liquid ring vacuum pump system.

A PLC-based SCADA system (IWS v7.1) provides real-time monitoring of key electrical and mechanical parameters through 4–20 mA analog and 24 VDC digital signal channels. The monitored parameters include turbine inlet and exhaust pressure, condenser vacuum level, steam mass flow rate, generator voltage and current, shaft rotational speed, vibration level, and auxiliary system status. The PLC continuously collects, processes, and archives operational data at 1-second intervals, enabling high-resolution performance tracking and transient event analysis during synchronization and load-following operations.

The archived dataset supports both long-term operational assessment and advanced control development. In particular, the high-frequency SCADA data were used to train and validate neural-network-based models for turbine inlet pressure control, improving system stability under fluctuating steam supply conditions. This integrated monitoring architecture ensures reliable plant supervision, facilitates early fault detection, and provides a robust data foundation for thermodynamic, electrical, and control-system performance evaluation.

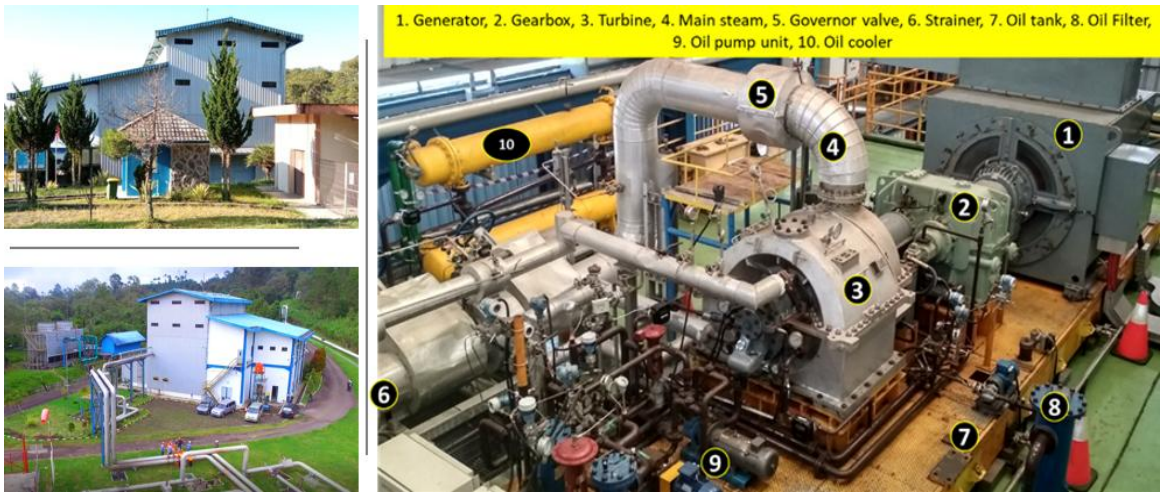

Figure 2. The powerhouse and turbine island of the 3 MW geothermal power plant

2.3. Testing protocol

The development of the 3 MW Kamojang geothermal pilot plant began in 2009–2010, followed by detailed engineering in 2010, component fabrication in 2011, and installation in 2013. Multi-phase testing was conducted under standardized procedures covering start-up, synchronization, and shutdown. Initial tests in 2014–2016 using a 500-kW dummy load confirmed stable mechanical operation. The first synchronization in 2018 delivered up to 1 MW for six hours, followed by 24-hour runs reaching 2.1 MW [10].

Synchronization tests on May 7–10, 2019, identified major performance constraints, notably a 0.4 bar(a) strainer pressure drop and elevated condenser pressure compared to the 0.16 bar(a) design, reducing turbine–generator efficiency to ~55% (design 69%). A 5×24-hour run in November 2019 delivered 526.41 MWh to the 20 kV PLN grid with a maximum net output of 2.05 MW. SCADA data as shown in Figure 3 confirmed stable operation but persistent vacuum limitations that prevented achieving the nominal 3 MW output. Reliability tests in 2021–2022 further verified operational continuity; however, condenser vacuum remained the primary factor constraining full-load performance.

2.4. Technical modification procedures

This study presents the systematic modification of a 2 MW backpressure turbine into a 3 MW condensing unit adapted to Kamojang's geothermal conditions. The redesign introduced six key upgrades: i) Sddition of a low-pressure sixth stage optimized for 162 °C and 6.5 bar(a); ii) Exhaust casing

reconfiguration for 0.16 bar(a) condenser operation with reduced turbulence; iii) Vacuum-compatible gland-seal and hybrid NCG removal system combining ejectors and a liquid-ring pump; iv) Strainer redesign cutting pressure drop from 0.4 bar to 0.02 bar; v) Condenser optimization through improved water distribution and hot-well-pump control; and vi) Gearbox coupling (6,543 rpm to 1,500 rpm) ensuring generator synchronization with minimal vibration. These integrated modifications demonstrate the technical feasibility of locally engineered, performance-optimized condensing turbines for small-scale geothermal applications.

Figure 3. The status of the final SCADA screen from the 3 MW power facility in the end of 2019

3. RESULT AND DISCUSSION

This section presents the quantitative results of the 3 MW Kamojang geothermal condensing pilot plant after sequential subsystem improvements, comparing the findings with both baseline data and existing international studies. The discussion emphasizes long-term performance, subsystem optimization, and exergy analysis.

3.1. Overview of performance improvement

From 2014 to 2022, with testing paused in 2020 due to COVID-19 and resumed in August 2021 following a condenser discharge-water setting adjustment, the Kamojang pilot demonstrated clear improvements in steam utilization, condenser performance, and system stability; Table 2 reports inlet-pressure +5.7%, condenser-pressure −11.6%, specific steam consumption (SSC) −4.7%, turbine isentropic efficiency +2.7 points, net power +7.8%, and exergy efficiency +2.1 points. These results are attributable to targeted subsystem redesigns—most notably the reduction in steam-strainer pressure drop (0.4→0.02 bar) and the stabilization of condenser vacuum—which increased turbine enthalpy drop and boosted output [15]. Mechanistically, optimized strainers minimize hydraulic losses and improve flow behavior [16], while condenser upgrades and effective NCG removal reduce exergy destruction and enhance efficiency, with impact magnitudes dependent on context [17], [18]. Consistent with broader evidence, long-term studies emphasize thermal-breakthrough dynamics and rigorous well management as prerequisites for maintaining performance over multi-year operations [19], [20].

Table 2. Summary of performance before and after subsystem modifications

Parameter	2019 (Pre-modification)	2021/22 (Post-modification)	Improvement
Inlet pressure (bar(a))	6.10	6.45	+5.7%
Condenser pressure (bar(a))	0.43	0.38	–11.6%
Specific steam consumption (SSC, t/MW)	14.56	13.87	–4.7%
Turbine isentropic efficiency (%)	63.4	66.1	+2.7 points
Net power output (MW)	2.05	2.21	+7.8%
Exergy efficiency (%)	71.5	73.6	+2.1 points

3.2. Condenser performance and NCG management

From 2019 to 2021/22, condenser pressure improved from 0.43 to 0.38 bar(a), an 11.6% reduction achieved through better condensate control and optimized LRVP operation [21]. As shown in Figure 4, the August 2021 synchronization test exhibited a lower and more stable condenser vacuum than the November

2019 test, indicating recovery after the period of inactivity during the pandemic. The 0.05 bar(a) vacuum improvement increased turbine enthalpy drop by approximately 7–8 kJ/kg, contributing to a ~3% rise in turbine efficiency. Remaining limitations are attributed to restricted condenser surface area and NCG accumulation, highlighting the need for enhanced heat-exchange capacity and hybrid ejector–LRVP upgrades [22].

Strainer improvements further supported turbine performance. Before modification, the strainer caused a 0.4 bar pressure drop, reducing effective steam supply to the turbine. After redesign, the pressure drop decreased to 0.02 bar, as shown in Figure 5, minimizing hydraulic losses and preventing particle deposition [23].

Long-term operation from November 16, 2021, to January 4, 2022, confirmed plant reliability. Removal of one restriction orifice increased turbine inlet pressure to 5.6 bar(g) (≈6.4 bar(a)), closer to the 6.5 bar(a) design target and significantly higher than the inlet pressures recorded during the 2019 tests (5.08 and 4.72 bar(g)). This improvement supports a larger enthalpy drop and more efficient turbine expansion.

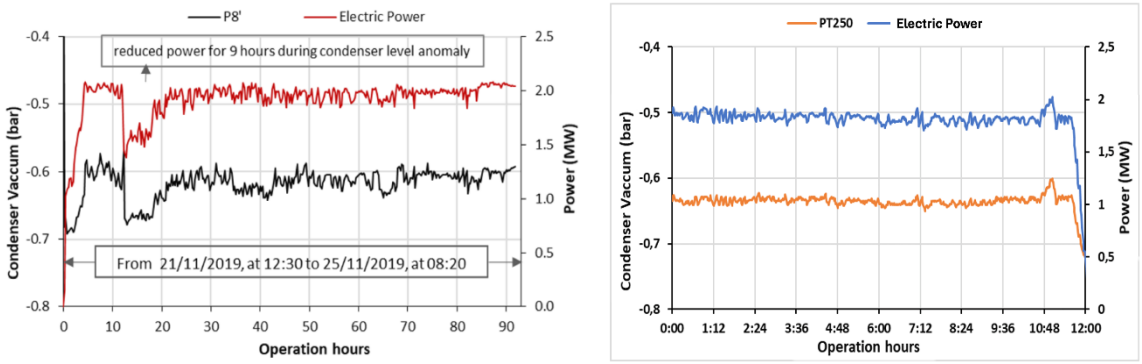

(a) (b)

Figure 4. Comparison test data result of November 2019 to August 2021: (a) running test data on November 2019 [16] and (b) running test data on August 2021.

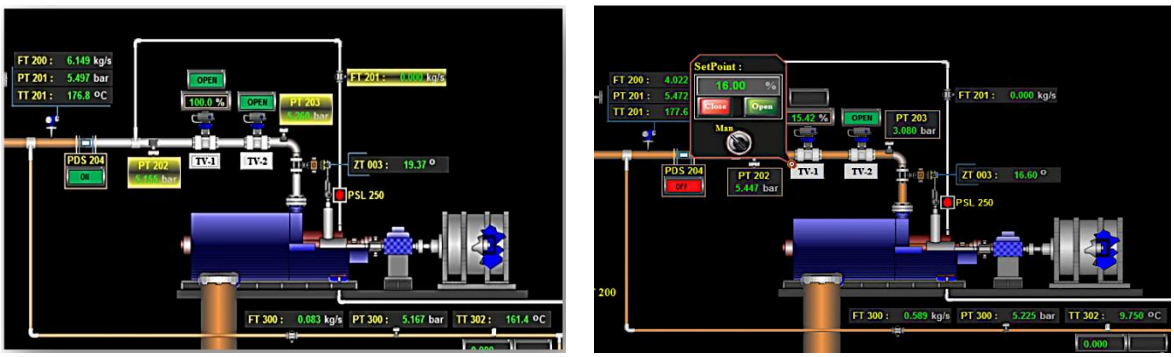

(a) (b)

Figure 5. The difference of the pressure drop in the strainer (pressure drop of PT-201 with PT-202): (a) in 2019, the pressure drop was 0.4 barg and (b) in 2021, after improvement, the pressure drop is 0.02 barg

3.3. Specific steam consumption (SSC) and power stability

Figure 6 compares turbine SSC data from the November 2019 and November 2021–January 2022 synchronization tests. The SSC decreased during the 2021–2022 period, indicating an improvement in turbine performance consistent with the reduced steam mass flow rate. SSC is defined as the ratio of steam mass flow to net power output, which depends on the enthalpy drop across the turbine. Increasing turbine inlet pressure and lowering exhaust pressure enhance this enthalpy drop, and the higher inlet pressure achieved during the latest tests reflects progress toward the design condition.

The plant's SSC design target is 9.12 t/MWh. Measured values were 13.92 t/MWh at 2.09 MW in 2019 and 14.56 t/MWh at 2.02 MW during 2021–2022, with the higher SSC largely influenced by condenser backpressure and off-design operating conditions.

Figure 7 shows that the turbine's isentropic efficiency (design: 73%) declined to 65% in 2019 and 63% in 2021. Contributing factors include steam property variations, insufficient condenser vacuum, and reduced enthalpy drop per stage. Additional losses in 2019 and 2021 were caused by turbine deposits, as no online washing facility was available. Although vibration levels increased in 2021, they remained within acceptable limits but contributed to a 100–200 kW reduction in turbine output. Despite improvements in condenser vacuum and strainer performance, these have not yet translated into a significant increase in turbine capacity.

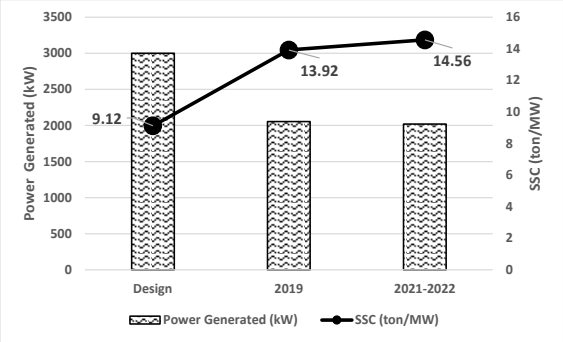

Figure 6. Comparison of turbine SSC data from synchronization experiments conducted in November 2019 and January 2021

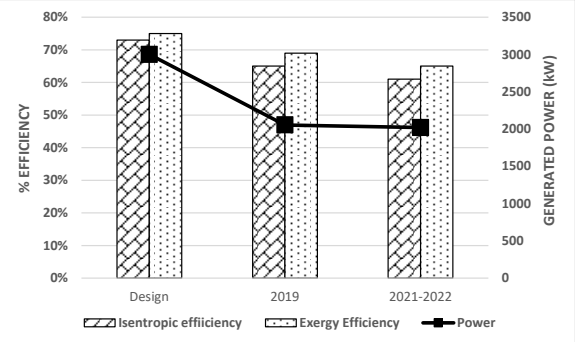

Figure 7. The comparison of the 3 MW Kamojang GPP's efficiencies

3.4. Electrical subsystem modeling and integration

3.4.1. System configuration and control architecture

The Kamojang 3 MW pilot GPP operates with a complete local-development electrical subsystem that integrates the generator, excitation system, protection relays, and synchronization controls into the overall supervisory automation network. The generator is a 4-pole, 3,750 kVA, 6.3 kV, 50 Hz brushless synchronous machine, directly coupled to a six-stage condensing steam turbine through a reduction gearbox (6485 to 1500 rpm). A Basler DEC-200 digital AVR performs voltage regulation, while a Woodward 2301D digital governor executes turbine speed and load control. Both controllers are interfaced through the GCP, which also hosts the GE Multilin SR-489 protection relay providing over/under-voltage, reverse-power, differential, and thermal protection logics. Additional ABB REF-610 relays protect the 6.3 kV and 20 kV feeders from current and voltage disturbances.

The generator is synchronized to the 20 kV Samarang feeder of PT PLN through a 6.3/20 kV step-up transformer, a vacuum circuit breaker (VCB), and a load-break switch (LBS) arrangement. This configuration was verified during witnessed grid synchronization testing by PLN Pusertif, confirming compliance with national interconnection standards and stable operation at 300–450 kW loading during the first commissioning phase [24]. PLN Pusertif is the accredited Certification Centre of PT PLN (Persero) responsible for ensuring conformity of electrical systems with national and international standards. The single diagram of the power plant is shown in Figure 8.

3.4.2. SCADA-based monitoring and remote supervision

The SCADA system, developed using SCADA IWS v7.1, serves as the backbone for the integrated operation of both mechanical and electrical subsystems. At the plant level, a PLC with redundant CPU and power supply collects real-time data from the GCP, Motor Control Centers (MCC 1 & 2), and field instruments through 24 VDC digital and 4–20 mA analog channels. Communication protocols combine OMRON Ethernet (OMETH) for PLC-to-SCADA links and Modbus TCP/IP for intelligent electronic devices such as the digital AVR, relay protection, load-sharing, and power-monitor modules. Four SCADA workstation monitors display turbine island, non-turbine island, alarm/trend, and instrumentation interfaces, providing complete situational awareness of generator voltage, current, frequency, and power factor. The SCADA system architecture of the 3 MW Kamojang geothermal power plant is shown in Figure 9. A SCADA Web Client innovation enables remote visualization at BRIN's head office (~250 km from Kamojang) with mirrored displays of the site system, allowing rapid decision-making during alarm events and operational diagnostics [25].

3.4.3. Intelligent pressure and load-following control

To enhance dynamic performance and reduce oscillations observed during initial synchronization, a new AI-based governor control approach was developed using neural-network backpropagation (BPNN) and non-linear autoregressive with exogenous input (NARX) models. Training data were derived from the SCADA archive (PT103 steam-pressure sensor input and ZT611 valve-position output) collected during turbine pressure control tests in August 2021. The optimized NARX model achieved MSE = 0.001 and 95.3% tracking accuracy, outperforming the baseline PID controller in maintaining the turbine-inlet pressure at 5.65±0.15 bar [26]. This intelligent control layer demonstrates the feasibility of integrating machine-learning algorithms with existing AVR and governor systems to realize adaptive load-following and frequency-stabilization functions compatible with smart-grid operation.

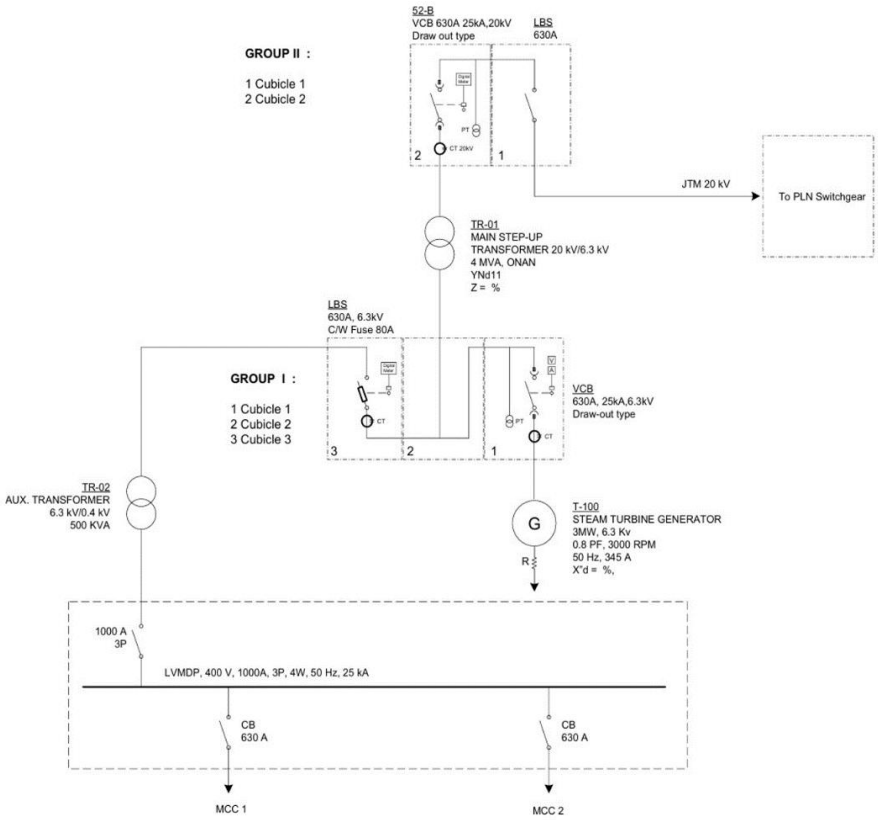

Figure 8. The 3 MW Kamojang geothermal power plant single line diagram [24]

3.5. Exergy analysis and irreversibility distribution

The extended exergy diagram as shown in Figure 10 illustrates the overall thermodynamic–electrical conversion pathway of the 3 MW Kamojang pilot plant. Of the total geothermal exergy input, mechanical irreversibilities at the separator (0.5%), inter-condenser (0.5%), turbine (9.5%), and main condenser (16.1%) account for 26.6%, while the remaining 73.6% is transferred to the electrical subsystem through the turbine–generator shaft. Within the electrical domain, additional losses arise from generator inefficiencies (≈2–4%), due to winding resistance, magnetic hysteresis, and ventilation, as well as auxiliary loads—cooling-water pumps, ejector–vacuum systems, and control instrumentation—consuming approximately 3% of gross electrical output. After these losses, the integrated system achieves a net exergy efficiency of about 71%, corresponding to the effective power delivered to the 20 kV PLN feeder. This combined thermodynamic–electrical representation provides a unified framework for assessing generator performance, auxiliary demand, and grid-coupled efficiency, and highlights improvement opportunities in turbine pressure control, generator excitation, and auxiliary system optimization.

3.6. Comparative and benchmark performance

Table 3 summarizes the performance of the Kamojang pilot plant relative to other small-scale geothermal units in Indonesia and abroad. The 3 MW Kamojang plant achieved a net output of 2.2 MW and

an SSC of 13.9–14.6 t/MWh—higher than the 9.12 t/MWh design target but comparable to similar installations. The remaining performance gap is primarily due to elevated condenser backpressure, auxiliary pressure losses, and the absence of online turbine cleaning. When compared with the Ulumbu 10 MW units (11–13 t/MWh), Kamojang demonstrates competitive performance within its scale class.

Internationally, the plant's exergy efficiency of 73.6% is consistent with small-scale units in Iceland, the Philippines, and Kenya, which typically employ advanced control strategies and hybrid configurations. These comparisons position Kamojang at an intermediate performance level—below large commercial systems but above many small-scale plants while indicating clear potential for further gains through condenser optimization, preventive maintenance, and subsystem integration [21], [27], [28].

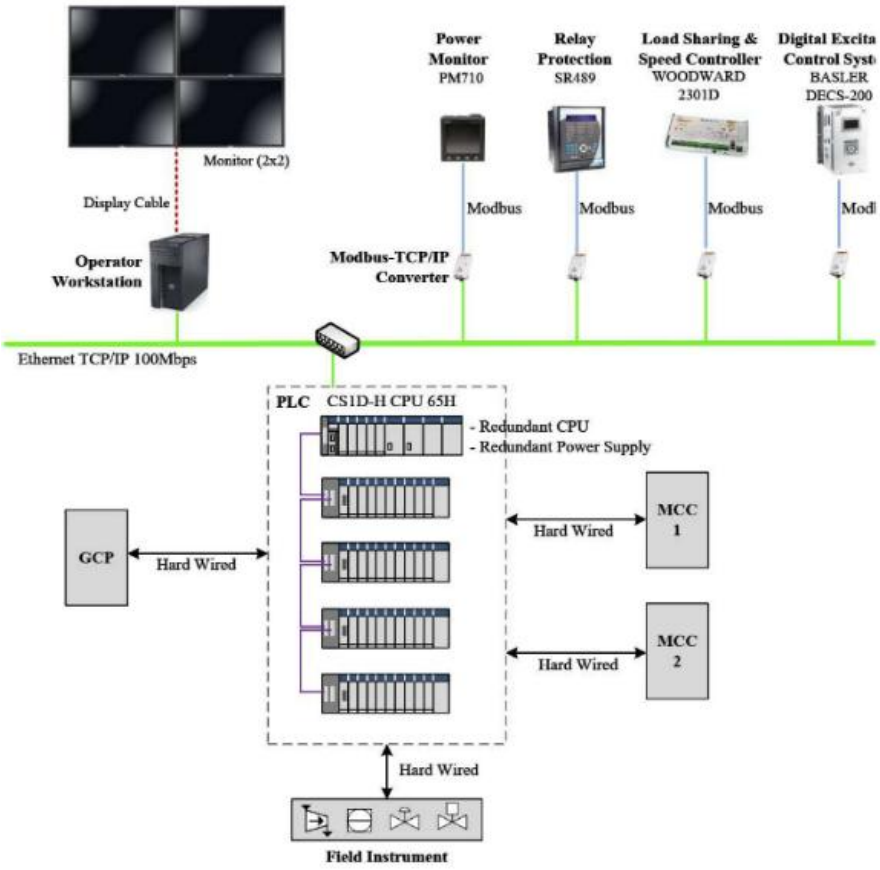

Figure 9. The 3 MW Kamojang geothermal power plant SCADA system architecture [25]

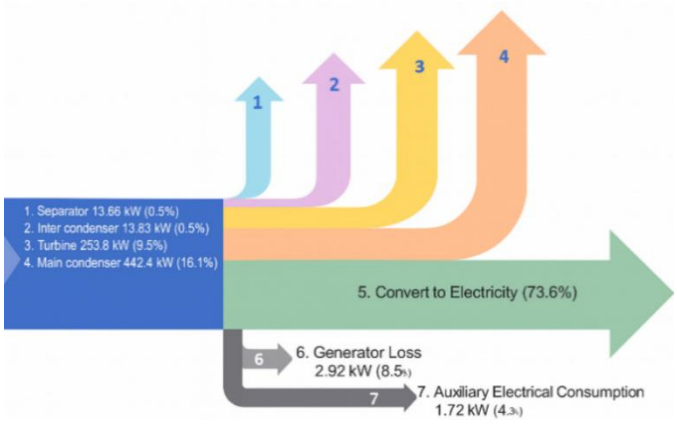

Figure 10. Sankey diagram of the exergy flow of the 3 MW Kamojang geothermal power plant

3.7. Error margins and SCADA reliability

To ensure the reliability of the performance indicators, error margins were evaluated for both SSC and exergy efficiency. Considering repeated measurements and sensor uncertainties, SSC was determined as 13.9–14.6 ±0.4 t/MWh (95% confidence), while exergy efficiency was 73.6±2.1%. These ranges reflect variations arising from turbine inlet pressure fluctuations, condenser vacuum instability, and occasional sensor drift.

SCADA data—central to long-term monitoring—were supported by routine calibration of pressure transducers, flow meters, and power measurement devices, with electrical outputs cross-validated against PLN grid data. Minor anomalies, such as drift in condenser water-level sensors and noise in vibration readings, were occasionally observed. These findings highlight the need for sensor redundancy and consistent calibration cycles, particularly in small-scale geothermal plants where modest measurement deviations can significantly influence reported efficiency values.

Table 3. Comparative and benchmark performance of small-scale geothermal units

No	Location / plant	Cycle type	Capacity (MW)	Condenser pressure (bar(a))	Exergy efficiency (%)	SSC (t/MWh)	Key technology feature	Reference
1	Kamojang, Indonesia	Condensing Steam	3.0	0.38 (design 0.16)	73.6	13.9–14.6 (design 9.12)	Hybrid NCG removal + SCADA	This study
2	Ulumbu, Indonesia	Condensing Steam	4 × 2.5 = 10.0	~0.12–0.15	71.2	~11–13	Modular turbine integration	Field data, 2023
3	Hellisheidi, Iceland	ORC-integrated Geothermal	5.0	0.34	72.0	–	Hybrid (Organic Rankine Cycles (ORC) efficiency enhancement	[29]
4	Tiwi, Philippines	Condensing Steam	3.5	0.37	74.1	–	Smart monitoring and hybrid energy mix	[21], [27]
5	Olkaria, Kenya	Multi-phase Extraction	2.8	0.35	72.4	–	Advanced turbine and extraction control	[28]

4. CONCLUSION

This study experimentally validated the operational performance of a locally engineered 3 MW condensing geothermal pilot plant under real field conditions. The 3 MW Kamojang geothermal pilot plant demonstrated the feasibility of a locally developed, reverse-engineered condensing turbine for small-scale applications. Improvements in strainer design and condenser operation reduced steam pressure losses, stabilized vacuum conditions, and enhanced SSC and exergy performance. Integration of the electrical subsystem including the 6.3 kV generator, digital AVR, governor, and SCADA monitoring confirmed stable grid operation and compliance with national standards. Accounting for 2–4% electrical losses and ~3% auxiliary consumption, the plant achieved a net exergy efficiency of 71%.

With 63.81% local content, the project highlights Indonesia's growing capability in geothermal technology localization. The operational lessons, particularly in condenser and NCG management, are transferable to 5–10 MW installations and support broader deployment of distributed geothermal systems. Overall, this study provides a unified thermodynamic–electrical evaluation framework and confirms the technical viability and scalability of small-scale condensing geothermal plants for Indonesia's clean-energy transition.

ACKNOWLEDGMENTS

The authors express gratitude to the Agency for the Assessment and Application of Technology (BPPT), which has been integrated into the National Research and Innovation Agency (BRIN) since 2021, for sponsoring this project and extend appreciation to the directors and management of PT. Pertamina Geothermal Energy (PGE) for their continuous assistance, which facilitated access to valuable data and field facilities for our research.

FUNDING INFORMATION

This research was funded by BPPT, which has been integrated into BRIN since 2021.

AUTHOR CONTRIBUTIONS STATEMENT

This journal uses the Contributor Roles Taxonomy (CRediT) to recognize individual author contributions, reduce authorship disputes, and facilitate collaboration.

Name of Author	C	M	So	Va	Fo	I	R	D	O	E	Vi	Su	P	Fu
Lina Agustina	✓	✓	✓	✓	✓	✓		✓	✓	✓	✓			
Suyanto		✓				✓		✓	✓	✓	✓	✓		
Budi Ismoyo						✓		✓		✓				

C : **C**onceptualization
M : **M**ethodology
So : **So**ftware
Va : **Va**lidation
Fo : **Fo**rmal analysis
I : **I**nvestigation
R : **R**esources
D : **D**ata Curation
O : Writing - **O**riginal Draft
E : Writing - Review & **E**diting
Vi : **Vi**sualization
Su : **Su**pervision
P : **P**roject administration
Fu : **Fu**nding acquisition

CONFLICT OF INTEREST STATEMENT

Authors state no conflict of interest.

DATA AVAILABILITY

The data that support the findings of this study are available from the corresponding author, [LA], upon reasonable request.

REFERENCES

[1] K. Piipponen *et al.*, "The deeper the better? a thermogeological analysis of medium-deep borehole heat exchangers in low-enthalpy crystalline rocks," *Geothermal Energy*, vol. 10, no. 1, p. 12, 2022, doi: 10.1186/s40517-022-00221-7.

[2] K. Rink *et al.*, "An environmental information system for the exploration of energy systems," *Geothermal Energy*, vol. 10, no. 1, p. 4, 2022, doi: 10.1186/s40517-022-00215-5.

[3] G. M. Idroes, I. Hardi, I. S. Hilal, R. T. Utami, T. R. Noviandy, and R. Idroes, "Economic growth and environmental impact: assessing the role of geothermal energy in developing and developed countries," *Innovation and Green Development*, vol. 3, no. 3, p. 100144, 2024, doi: 10.1016/j.igd.2024.100144.

[4] H. Alhusni, T. Satria, P. Perdana, E. H. Purwanto, and H. Setyawan, "Geothermal business outlook in Indonesia," in *48th Workshop on Geothermal Reservoir Engineering Stanford University*, Stanford, CA, USA, 2023, pp. 1–12.

[5] N. A. Pambudi and D. K. Ulfa, "The geothermal energy landscape in Indonesia: a comprehensive 2023 update on power generation, policies, risks, phase and the role of education," *Renewable and Sustainable Energy Reviews*, vol. 189, p. 114008, 2024, doi: 10.1016/j.rser.2023.114008.

[6] S. W. Yudha, B. Tjahjono, and P. Longhurst, "Unearthing the dynamics of Indonesia's geothermal energy development," *Energies*, vol. 15, no. 14, p. 5009, 2022, doi: 10.3390/en15145009.

[7] U. Azmi *et al.*, "A holistic overview: Indonesia's geothermal energy encourages geothermal power plant investment in support of national defense," *Jurnal Pertahanan dan Bela Negara*, vol. 14, no. 2, pp. 132–150, 2024, doi: 10.33172/jpbh.v14i2.19624.

[8] C. M. Sufyana, F. T. Akbar, and W. Srigutomo, "Thermal modeling and simulation of a single-flash geothermal power plant involving non-condensable gas: a case study of Kamojang geothermal field in Garut, West Java, Indonesia," *Geothermal Energy*, vol. 11, no. 1, 2023, doi: 10.1186/s40517-023-00249-3.

[9] B. Rudiyanto, A. Wicaksono, and M. Hijriawan, "Evaluation and optimization based on exergy in Kamojang geothermal power plant unit 3," *International Journal on Advanced Science, Engineering and Information Technology*, vol. 13, no. 6, pp. 2372–2379, 2023, doi: 10.18517/ijaseit.13.6.19441.

[10] B. T. Prasetyo, Suyanto, M. A. M. Oktaufik, and H. Sutriyanto, "Testing of early stage of bppt-3mw condensing type small scale geothermal power plant - Kamojang - Indonesia," in *Journal of Physics: Conference Series*, IOP Publishing, 2019, p. 12014, doi: 10.1088/1742-6596/1376/1/012014.

[11] B. Rudiyanto, M. S. Birri, Widjonarko, C. Avian, D. M. Kamal, and M. Hijriawan, "A genetic algorithm approach for optimization of geothermal power plant production: case studies of direct steam cycle in Kamojang," *South African Journal of Chemical Engineering*, vol. 45, pp. 1–9, 2023, doi: 10.1016/j.sajce.2023.04.002.

[12] M. Aziz and F. B. Juangsa, "Dry steam power plant: thermodynamic analysis and system improvement," in *Thermodynamic Analysis and Optimization of Geothermal Power Plants*, Elsevier, 2021, pp. 97–111, doi: 10.1016/B978-0-12-821037-6.00015-9.

[13] X. Chen, Z. Tian, F. Guo, X. Yu, and Q. Huang, "Experimental investigation on direct-contact condensation of subatmospheric pressure steam in cocurrent flow packed tower," *Energy Science and Engineering*, vol. 10, no. 8, pp. 2954–2969, 2022, doi: 10.1002/ese3.1181.

[14] B. T. Prasetyo, Suyanto, Cahyadi, and H. Sutriyanto, "Lesson learned – the operation of the pilot scale geothermal power plant 3mw – Kamojang, Indonesia," *Geothermics*, vol. 91, p. 102025, 2021, doi: 10.1016/j.geothermics.2020.102025.

[15] C. Ding, X. Zhang, G. Liang, and J. Feng, "Optimizing exergy efficiency in integrated energy system: a planning study based on industrial waste heat recovery," *IEEE Access*, vol. 12, pp. 148074–148089, 2024, doi: 10.1109/ACCESS.2024.3468291.

[16] G. P. Mahajan and R. S. Maurya, "Development of an efficient t-type strainer with its performance evaluation," *Journal of Thermal Engineering*, vol. 6, no. 6, pp. 420–433, 2020, doi: 10.18186/THERMAL.836499.

[17] Z. Wang, "Advancements in geothermal energy: extraction methods, utilization practices, and future improvements," *Applied and Computational Engineering*, vol. 98, no. 1, pp. 149–156, 2024, doi: 10.54254/2755-2721/98/2024fmceau0104.

[18] G. Mittal, N. G. Malik, A. Bhuvanendran Nair Jayakumari, D. Martelo, N. Kale, and S. Paul, "Spray parameters and coating microstructure relationship in suspension plasma spray tio2 coatings," *Coatings*, vol. 13, no. 12, p. 1984, 2023, doi: 10.3390/coatings13121984.
[19] I. R. Kivi, E. Pujades, J. Rutqvist, and V. Vilarrasa, "Cooling-induced reactivation of distant faults during long-term geothermal energy production in hot sedimentary aquifers," *Scientific Reports*, vol. 12, no. 1, 2022, doi: 10.1038/s41598-022-06067-0.
[20] F. S. Tut Haklıdır, "The importance of long-term well management in geothermal power systems using fuzzy control: a western Anatolia (Turkey) case study," Energy, vol. 213, p. 118817, Dec. 2020, doi: 10.1016/j.energy.2020.118817.
[21] D. Fiaschi, G. Manfrida, B. Mendecka, L. Tosti, and M. L. Parisi, "A comparison of different approaches for assessing energy outputs of combined heat and power geothermal plants," *Sustainability (Switzerland)*, vol. 13, no. 8, p. 4527, 2021, doi: 10.3390/su13084527.
[22] R. S. Kusumo, D. Rhakasywi, and F. Fahrudin, "Analysis of allergies and optimization in Kamojang dry steam type geothermal power plant with a capacity of 55 mw," *Eduvest - Journal of Universal Studies*, vol. 4, no. 12, pp. 11695–11707, 2024, doi: 10.59188/eduvest.v4i12.44733.
[23] P. Ungar, Z. Özcan, G. Manfrida, Ö. Ekici, and L. Talluri, "Off-design modelling of orc turbines for geothermal application," in *E3S Web of Conferences*, 2021, p. 11015. doi: 10.1051/e3sconf/202131211015.
[24] R. Hartadhi, S. Budi Prasetyo, A. Prastawa, and T. Surana, "Grid synchronization test of the local development 3 mw geothermal power plant," *4th IEEE Conference on Power Engineering and Renewable Energy, ICPERE 2018 - Proceedings*. 2018. doi: 10.1109/ICPERE.2018.8739667.
[25] J. Prihantoro, H. Taufiqurrohman, Suyanto, Cahyadi, A. Larasati, and A. Nurrohim, "Implementation of SCADA web client for monitoring geothermal power plant 3 MW Kamojang - Indonesia," in *Proceedings - 2022 2nd International Conference on Electronic and Electrical Engineering and Intelligent System, ICE3IS 2022*, 2022, pp. 270–275. doi: 10.1109/ICE3IS56585.2022.10010311.
[26] J. Prihantoro *et al.*, "Performance pressure control system for inlet turbine using neural network backpropagation and narx model in the geothermal power plant 3 mw kamojang-indonesia," in *AIP Conference Proceedings*, 2024. doi: 10.1063/5.0205821.
[27] L. Kumar, M. S. Hossain, M. E. H. Assad, and M. U. Manoo, "Technological advancements and challenges of geothermal energy systems: a comprehensive review," *Energies*, vol. 15, no. 23, p. 9058, 2022, doi: 10.3390/en15239058.
[28] A. K. Bett and S. Jalilinasrabady, "Optimization of orc power plants for geothermal application in kenya by combining exergy and pinch point analysis," *Energies*, vol. 14, no. 20, p. 6579, 2021, doi: 10.3390/en14206579.
[29] Y. Tranamil-Maripe, J. M. Cardemil, R. Escobar, D. Morata, and C. Sarmiento-Laurel, "Assessing the hybridization of an existing geothermal plant by coupling a csp system for increasing power generation," *Energies*, vol. 15, no. 6, p. 1961, Mar. 2022, doi: 10.3390/en15061961.

BIOGRAPHIES OF AUTHORS

Lina Agustina works as a researcher in the Research Center for Energy Conversion and Conservation, National Research and Innovation Agency of the Republic of Indonesia. She received a master's degree in geothermal engineering from the Bandung Institute of Technology (ITB) in 2013. She specializes in the thermodynamics of steam power plants, ORC power plants, sustainable energy conversion, and refrigeration systems. She can be contacted at email: lina007@brin.go.id.

Suyanto is a researcher at the Research Center for Energy Conversion and Conservation Energy under the National Research and Innovation Agency (BRIN) in Indonesia. He received his Bachelor of Engineering in Mechanical Engineering from the Aachen University of Applied Sciences, Germany, in 1996 and his Master of Electrical Engineering from Curtin University of Technology, Australia, in 2002. His expertise is in energy, equipment technology, and energy systems, especially geothermal technology. He can be contacted at email: suya006@brin.go.id.

Budi Ismoyo is a researcher in the Research Center for Energy Conversion and Conservation at the National Research and Innovation Agency (BRIN), Serpong, Indonesia. He received his bachelor's degree and master's degree from Universitas Brawijaya and Universitas Indonesia in 2008 and 2021. He has been an engineering staff member at BRIN, Serpong, Indonesia, since 2010. He is currently an engineer in the field of thermal simulation. His research interests include small-scale power plant design and prototyping of thermal systems for industrial applications. Evaluation of chillers, boilers, cooling towers, and processes in terms of energy is his specialty. He can be contacted at email: budi049@brin.go.id.